Available online at www.sciencedirect.com

ScienceDirect

Procedia Engineering 126 (2015) 315 – 320

Procedia Engineering

www.elsevier.com/locate/procedia

7th International Conference on Fluid Mechanics, ICFM7

Simulation of flows through submerged vegetation patches using macroscopic turbulence models

Zhiya Chen[a,b], C.W. Li[a]*, Jiemin Zhan[b]

[a]*Department of Civil and Environmental Engineering, The Hong Kong Polytechnic University, Hong Kong, China*
[b]*School of Engineering, Sun Yet-Sen University, Guangzhou, China*

Abstract

Macroscopic approach incorporating the spatial averaging procedure is commonly used to investigate turbulent flows in porous media, terrestrial and aquatic canopies. In this work the hydrodynamics of flows through a semi-rigid vegetation patch (VP) was investigated with two macroscopic turbulence models. We modified the Reynolods Averaged Navier Stokes (RANS) equations to obtain the Volume Averaged (VARANS) equations and performed simulations using the open source code OpenFOAM. The numerical results of gradually varied flows over submerged VPs are compared with the corresponding experimental measurements. The results show that the macroscopic turbulence models simulate the velocity profiles with acceptable accuracy. The increase of vegetation density generates higher Reynolds stress around the top of vegetation and smaller velocity inside the VP. The two models perform differently in the computation of Reynolds stress, with the profiles from the model of Uittenbogaard (2003) requiring a shorter distance to reach the uniform state for the case of low vegetation density. Further works will be carried out to identify the cause of difference and to achieve a refined macroscopic turbulence model.

Peer-review under responsibility of The Chinese Society of Theoretical and Applied Mechanics (CSTAM)

Keywords: turbulence model; vegetation patch; OpenFOAM;

1. Introduction

In aquatic ecosystems, submerged vegetation patches (VPs) play an important role, including baffling of local currents, dampening of wave energy, and providing food and shelter to many organisms. VPs also affect the

* Corresponding author. Tel.:852-27666043; fax:852-23346389.
E-mail address: cecwli@polyu.edu.hk

Peer-review under responsibility of The Chinese Society of Theoretical and Applied Mechanics (CSTAM)
doi:10.1016/j.proeng.2015.11.194

sedimentation and erosion processes by creating regions of increased or decreased bed shear stresses and can increase habitat and species diversity. The major impact of vegetation on flood protection and ecological management is the reduction of flow velocity and the increase of water depth.

Experiments about the effects of variations in species and VP configuration on the fluid dynamics of flows over vegetation were reviewed in [1]. Bouma et al.[2] combined field, flume and numerical experiments to identify spatial sedimentation and erosion patterns within VPs.

For aquatic canopy flows, numerical modelling was generally carried out for fully-developed flows over submerged vegetation based on the macroscopic approach. The volume (spatially)-averaged Reynolds-averaged Navier–Stokes (VARANS) equations [1] were developed [3] through averaging the RANS equations over a representative elementary volume [3][4]. The additional volume averaged correlation terms generated are modeled by various turbulence closures [5][6][7].

In this work the turbulent flow over a submerged VP in an open channel is studied numerically using two models of k- ε type. The computed results are compared with the corresponding laboratory data of Bouma et al.[2]. The mechanisms controlling the turbulent development inside a VP are also discussed. These turbulence models have been tested for fully-developed vegetated flow while their performance in turbulent transitional flow over a finite VP has not been reported.

2. Macroscopic approach: VARANS equations and VA turbulence models

2.1 VARANS equations

The VARANS equations describe the flow within a VP through the volume averaging of the RANS equations. Details on the additional terms resulting from the volume averaged (VA) procedure are given by Souliotis and Prinos (2011). For steady flow over rigid vegetation

$$\frac{\partial \langle U_i \rangle}{\partial x_i} = 0 \tag{1}$$

$$\langle U_j \rangle \frac{\partial \langle U_i \rangle}{\partial x_i} = -\frac{1}{\rho}\frac{\partial \langle P \rangle}{\partial x_i} - \frac{\partial}{\partial x_j}\langle \overline{u_i u_j} \rangle - \frac{\partial}{\partial x_j}\langle U_i U_j \rangle + S_{mi} \tag{2}$$

where U_i denotes velocity components, x_i denotes spatial ordinates, P denotes pressure, u_i denotes temporal fluctuation of velocity component, the symbol $\langle\ \rangle$ indicates spatial averaging and the symbol ~ indicates spatial fluctuations. The last term S_{mi} describing form and viscous drags is modelled based on medium type (porous or vegetation). In the regions upstream, above and downstream of the VP, the extra source terms vanish and the governing equations are simplified to the RANS equations.

2.2 Turbulence transport equations

The transport equations for turbulent kinetic energy $\langle k \rangle$ and dissipation rate $\langle \varepsilon \rangle$ is based on VA of the original transport equations for k and ε. The transport equation for k is

$$\langle U_j \rangle \frac{\partial \langle k \rangle}{\partial x_j} = \frac{\partial}{\partial x_j}\left(\frac{\langle \nu_t \rangle}{\sigma_\kappa}\frac{\partial \langle k \rangle}{\partial x_j} \right) - \left(\langle u_i u_j \rangle \frac{\partial \langle U_i \rangle}{\partial x_j} \right) - \langle \varepsilon \rangle + S_k \tag{3}$$

where S_k is an additional production term of the turbulent kinetic energy due to the turbulence energy production by vegetation. Its parameterization is shown in Table 1. Similarly, the transport equation for $\langle \varepsilon \rangle$ is

$$\langle U_j \rangle \frac{\partial \langle \varepsilon \rangle}{\partial x_j} = \frac{\partial}{\partial x_j}\left(\frac{\langle \nu_t \rangle}{\sigma_\varepsilon}\frac{\partial \langle \varepsilon \rangle}{\partial x_j} \right) - c_{\varepsilon 1}\frac{\langle \varepsilon \rangle}{\langle k \rangle}\left(\langle u_i u_j \rangle \frac{\partial \langle U_i \rangle}{\partial x_j} \right) - c_{\varepsilon 2}\frac{\langle \varepsilon \rangle^2}{\langle k \rangle} + S_\varepsilon \tag{4}$$

where S_ε is the additional production of dissipation due to vegetation. Its parameterization is showed in Table 1. In Table 1, ν is the kinematic viscosity, ϕ is the porosity, K is the permeability equal to $(C_d\alpha)^{-2}$, C_d is the drag coefficient, α is the spatial density of vegetation, A_p is the solidity, t_{eff} is a time scale based on the vegetation and turbulence characteristics [7], C_f, C_k, C^2 are empirical constants.

Table 1 Extra source terms in Eqs. (2), (3)and(4)

Source terms	Pedras and de Lemos	Uittenbogaard
S_{mi}	$-\left(\frac{\nu\phi}{K}\right)\langle U_i\rangle-\left(\frac{c_f\phi^2}{\sqrt{K}}\right)\lvert\langle U\rangle\rvert\langle U_i\rangle$	$-0.5C_d\alpha\frac{1}{1-A_p}\lvert\langle U\rangle\rvert\langle U_i\rangle$
S_k	$\frac{c_k\phi^2}{\sqrt{K}}\lvert\langle U\rangle\rvert\langle k\rangle$	$-0.5C_d\alpha\lvert\langle U\rangle\rvert\langle U\rangle^2$
S_ε	$\frac{c_2c_k\phi^2}{\sqrt{K}}\lvert\langle U\rangle\rvert\langle\varepsilon\rangle$	$-0.5C_d\alpha t_{eff}^{-1}\lvert\langle U\rangle\rvert\langle U\rangle^2$

3. Numerical cases setup

The open source code OpenFoam 2.3.0 was used to solve the Equations (1)-(4). The stander $k-\varepsilon$ model and the standard solver pisoFoam were modified accordingly to incorporate the additional source terms for each model. For the solution algorithm, the Euler scheme was used for ddtSchemes, the Gauss linear scheme is used for laplacianSchemes, gradSchemes and divSchemes, and the linear scheme is used for interpolationSchemes. The 2D grid system was orthogonal and structured, formed by using GAMBIT. Grid-independence tests have been performed to ensure that the discretization error is small.

For boundary conditions at the inlet the velocity is specified, at the outlet the pressure is fixed. At the free surface the rigid-lid assumption is used and symmetry boundary conditions are specified. At the bed and side boundaries the wall function is applied (Fig. 1).

The experiment was conducted in a 10.8 m long and 0.6 m wide flume for a flow depth of 0.40 m. The VP length was 2 m with the vegetation simulated by vertical rigid cylinders of 0.007 m diameter and 0.20 m height. Plant densities were α =0.175 m^{-1} and 2.8 m^{-1}, while mean velocity was U_m=0.33 m/s. For all the cases listed in Table 2, C_d=1 was used. The canopy is considered dense for $C_d\alpha h>0.1$ and sparse for $C_d\alpha h<0.1$.

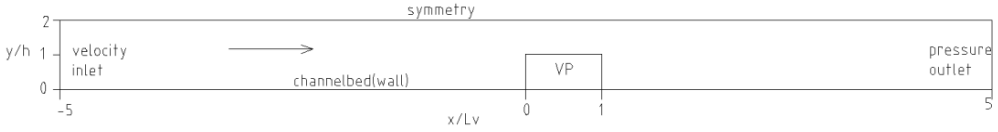

Fig. 1 Computational domain and setup of cases 1 and 2

Table 2 Cases studied

Cases	$\alpha(m^{-1})$	$L_v(m)$	$C_d\alpha h(-)$	Vegetation type
1	0.175	2	0.035	Sparse
2	2.8	2	0.56	Dense

4. Analysis of results

4.1 General

The computed results are shown in Fig. 2 and Fig. 3. The distance y is measured from the channel bed, the vegetation height h equals to 0.2 m and the vegetation length L_v equals to 2m. Three locations along the flume were

selected for comparison with the experimental data. The first is at the upstream of the VP ($x/L_v = -0.1$), the other two are within the VP ($x/L_v = 0.025$, $x/L_v = 0.9$).

4.2 Velocity and Reynolds stress profiles

The velocity profiles at different locations are showed in Fig.2. The velocity profiles at upstream of VP match the experimental data well. For sparse VP (Case 1), the computed velocity profiles have a weak inflection point along the VP. Inside VP, the computed values are higher indicating the drag due to vegetation is lower as compared to that of the test data. For dense VP (Case 2), the profiles in the vegetation region reveal a strong inflection point along the VP. Inside the VP, lower velocity is computed as compared with the sparse case due to the increased drag from the VP. Both profiles are however similar and do not reach the uniform state.

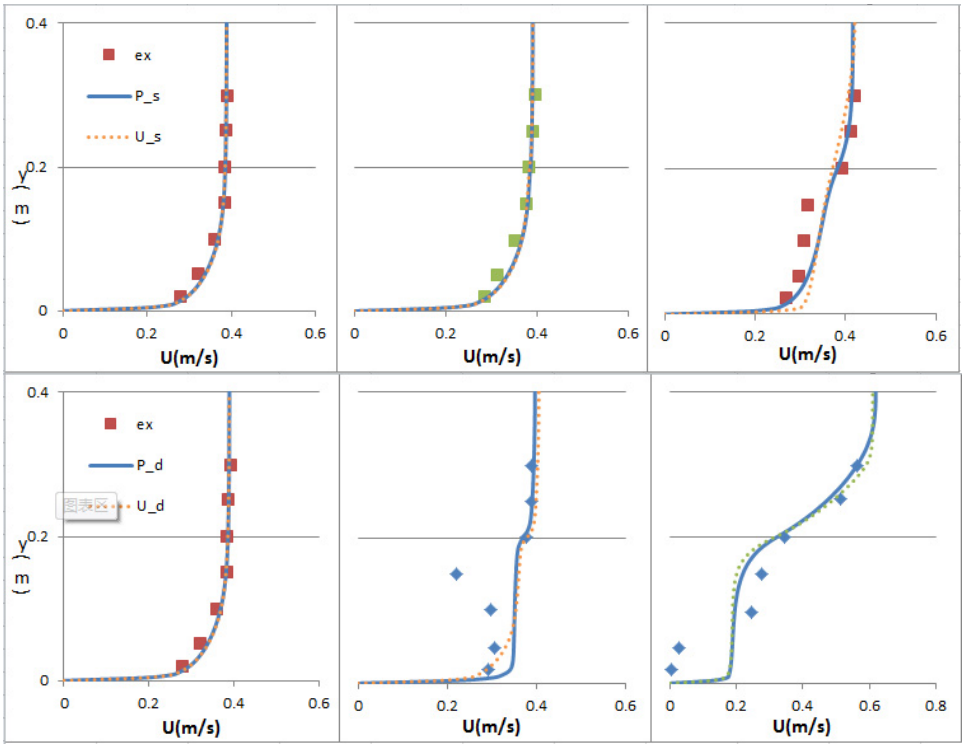

Fig.2. Vertical distributions of $\langle U_x \rangle$ along sparse (Case 1) and dense (Case 2) VP for L_v=2 m. The first is located at $x/L_v = -0.1$, the second is at $x/L_v = 0.025$, the last is at $x/L_v = 0.9$.

Figure 3 shows the vertical profiles of the Reynolds stress. For the sparse case, high values of the stress are computed within the VP. The computed results show that at the regions of large velocity gradient (the channel bed and the canopy top) the Reynolds stress is the largest, especially for the case of dense vegetation. Comparing the results of the two models, the Reynolds stress profiles computed by the Uittenbogaard model have higher values near the canopy top for the case with low vegetation density, indicating that they need a shorter distance to reach the uniform state. The cause of the difference is not known and will be studied in the future work.

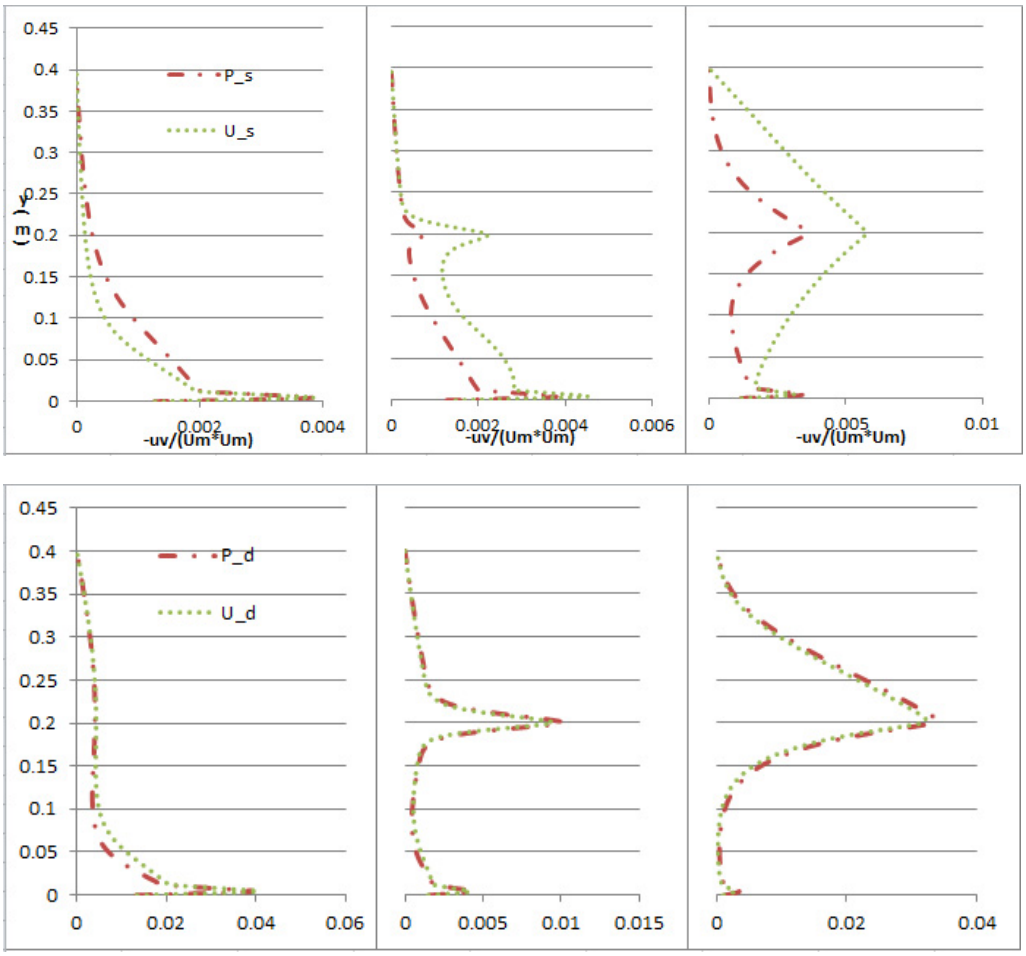

Fig. 3. Vertical profiles of Reynolds stress -$\langle\overline{u_1 u_3}\rangle$ normalized by U_m^2 along sparse (Case 1) and dense (Case 2) VP for L_v=2 m. The first is located at $x/L_v = -0.1$, the second is at $x/L_v = 0.025$, the last is at $x/L_v = 0.9$.

5. Conclusions

The effect of a VP on turbulent channel flow has been numerically studied using two models of $k-\varepsilon$ type. The computed results are compared with available experimental data. From the numerical results, an increase of the vegetation density causes higher Reynolds stress near and above the top of vegetation and smaller velocity inside the VP. The computed Reynods stress profile by the model of Uittenbogaard (2003) needs a shorter distance to reach the uniform state for the case of low vegetation density, as compared to that computed by the model of Pedras and de Lemos (2001). Further works will be carried out to identify the cause of difference and to achieve a refined macroscopic turbulence model.

Nomenclature

c_1	constant (–)
c_f	Forchheimer coefficient (=0.55)
c_k, c_2	constants (=0.28, 1.9)
C_d	drag coefficient
$C_{pw,} C_{\varepsilon w}$	constants (=0.8, 4.0)
$C_{p\varepsilon w}, C_{D\varepsilon w}$	constants (=1.5, 3.24)
t_{eff}	variable based on geometrical and turbulence characteristics (1/s)

References

[1]. Finnigan, J. Turbulence in plant canopies. *Annual Review Fluid Mech*.32(2000) 519–571

[2]. Bouma, T.J., van Duren, L.A., Temmerman, T.,et al..Spatial flow and sedimentation patterns within patches of epibenthic structures: Combining field, flume and modelling experiments. *Continental Shelf Res*. 27(2007) 1020–1045

[3]. Whitaker, S. *The method of Volume Averaging*. Kluwer, Dordrecht NL. (1999).

[4]. Slattery, J.C. Advanced Transport Phenomena. *Cambridge Univ. Press*, Cambridge, UK. (1999).

[5]. Foudhill, H., Brunet, Y., Caltagirone, J.-P. A fine-scale $k-\varepsilon$ model for atmospheric flow over heterogeneous landscapes. *Env. Fluid Mech*.5(2005) 247–265.

[6]. Pedras, M.H.J., de Lemos, M.J.S.. Macroscopic turbulence modelling for incompressible flow through undeformable porous media. *Int. J. Heat and Mass Transfer* 44(2001)1081–1093.

[7]. Uittenbogaard, R. Modelling turbulence in vegetated aquatic flows. Workshop Riparian Forest Vegetated Channels. Trento, Italy, 1–17. (2003).